ON THE STRUCTURE AND PHYSICAL ORIGIN OF THE WEAK INTERACTION BETWEEN H AND CO

Vladimír Lukeš[a1], Viliam Laurinc[a2,*], Michal Ilčin[a3] and Stanislav Biskupič[b]

[a] *Department of Chemical Physics, Slovak University of Technology, Radlinského 9, SK-812 37 Bratislava, Slovak Republic; e-mail:* [1] *vladimir.lukes@stuba.sk,* [2] *viliam.laurinc@stuba.sk,* [3] *michal.ilcin@stuba.sk*

[b] *Department of Physical Chemistry, Slovak University of Technology, Radlinského 9, SK-812 37 Bratislava, Slovak Republic; e-mail: stanislav.biskupic@stuba.sk*

Received May 22, 2003
Accepted July 3, 2003

Dedicated to Professor Rudolf Zahradník on the occasion of his 75th birthday.

The adiabatic potential energy surface of the H–CO complex in the van der Waals region, described by Jacobi coordinates (r = 1.128 Å, R, Θ), was investigated using the supermolecular coupled-clusters CCSD(T) method. Our calculations indicate a minimum for bent arrangements. It was found on the carbon side of CO molecule at R = 3.6 Å (Θ = 76°) with a well depth of D_e = –156.5 μE_h. The saddle points are localised at linear conformations for R = 4.37 Å (Θ = 0°) and R = 3.91 Å (Θ = 180°). The physical origin of the studied interaction was analysed by the intermolecular perturbation theory based on the single-determinant unrestricted Hartree–Fock wave function. The separation of the interaction energies shows that the locations of the predicted stable bent structure is primarily determined by delicate balance between the repulsive Heitler–London and attractive dispersion and induction energy components.

Keywords: Interaction energy; Potential energy surface; H–CO; van der Waals complex; Intermolecular perturbation theory; Coupled clusters; CCSD(T) method; *Ab initio* calculation.

Intermolecular systems involving carbon monoxide are actually of interest not only from the point of view of the combustion processes but also from the point of view of basic research[1,2]. In chemistry of interstellar molecules the reaction of hydrogen with carbon monoxide and formation of formyl radical is assumed to be an important step in the synthesis of oxygenated organic molecules[3–5]. The hydrogen radical reaction with carbon monoxide and dissociation of HCO was investigated in numerous computational studies and large effort was devoted to the study of the structure, electronic and vibrational energies of HOC and HCO [6–19].

The first global *ab initio* potential energy surface (with only small semi-empirical adjustment) was elaborated by Bowman, Bittman and Harding (BBH)[4] and used in the studies of the bound vibrational states. The dynamic studies in which the potential energy surface (PES) of BBH was used predicted quantitatively correctly the available experimental data. On the portion of the HCO surface investigated they found three minima corresponding to HCO, HOC and H + CO and five saddle points. List of references of the time-dependent dynamic calculations of Bowman and co-workers can be found in latter papers of that group[9–11]. Extensive *ab initio* calculations of the bending and C–O stretching PES for low-lying doublet electronic states for the HCO radical were reported by Lorenzen-Schmidt *et al.*[12]

The more accurate PES of Werner and co-workers[13] is a PES based on calculations performed at the multireference configuration interaction level (MRCI) level using complete active space self consistent field (CASSCF) reference functions and a basis set of quadruple zeta quality. The resonance energies and widths obtained from dynamics calculations based on this PES agree very well with the experimental data[13,14]. An extended list of previous experimental and theoretical studies can be also found in these papers. Structure, stability, and harmonic vibrational frequencies of stationary points for the HCO radical in the ground (^{2}A′) and first excited (^{2}A″) states were calculated by Bittererová *et al.*[15] Among recent *ab initio* calculations, it is worth mentioning the benchmark study of Woon[16], where the H + CO reaction has been described using correlation-consistent basis sets at five levels of theory. The predictions of the RCCSD(T) method were found close to those of the MRCI+Q method. Hybrid density functional theory (DFT) methods used by Jursic[17] predicted results of a similar quality to MRCI with Q/cc-pVQZ basis sets for resonances, but offered quite a different transition state structure and very low reaction barriers. To the best of our knowledge, in the previous *ab initio* studies no special attention was focused on the detailed calculation of the PES in the van der Waals region, especially either the grid used was not sufficient or the PES has been calculated only near the equlibrium geometries[18,19]. However, these weak bound van der Waals (vdW) systems might be prereactive complexes formed in the entrance valleys of PES.

With respect to previous theoretical works, the main goal of this paper is threefold: (i) to provide the detailed and improved basis set superposition error (BSSE)-corrected[20,21] characterisation of the PES of the H–CO complex at the supermolecular coupled-clusters theoretical level, (ii) to present the fitted functional form of the obtained *ab initio* results and (iii) to analyse

the origin of the anisotropy and stability of stationary points on PES by the intermolecular perturbation theory.

METHODOLOGY AND DEFINITIONS

In order to investigate the weak interaction within the radical vdW system, we will use the standard *ab initio* supermolecular approach[22–25]. At a given level of perturbation or CCSD(T) theory, the interaction energy is calculated from the expression:

$$\Delta E_{\mathrm{int}}^{(n)} = E_{\mathrm{AB}}^{(n)} - E_{\mathrm{A}}^{(n)} - E_{\mathrm{B}}^{(n)} \qquad n = \mathrm{HF},\ 2,\ 3,\ 4,\ \ldots \text{ or } \mathrm{CCSD(T)}\,, \tag{1}$$

where E_{AB} is the energy of the supersystem AB, and E_{A} (E_{B}) stands for the energy of the non-interacting monomer A (B). The level of theory is indicated by the superscript "*n*", *e.g.* $\Delta E_{\mathrm{int}}^{(2)}$ denotes the MP2 interaction energy.

To analyse the supermolecular results, the interpretation tools based on the intermolecular perturbation theory (I-PT) are applied at the SCF as well as at post-HF levels of theory[26–29]. In the case of the open-shell systems, the interaction energy contributions can be calculated in the framework of single-determinant restricted Hartree–Fock (RHF) and/or unrestricted Hartree–Fock (UHF) approaches[30–33]. In spite of some advantages, their application is associated with certain problems. In general, the Hamiltonian matrix elements provided by the RHF solutions for radical monomers are not invariant to the arbitrary orthogonalisation procedure. On the other hand, the use of UHF wave function is associated with difficulties resulting from its spin contamination. If this contamination is not serious, I-PT based on the UHF determinant is conceptually more straighforward than that based on the RHF determinant because of the presence of an additional one-particle operator[30,31].

The UHF–SCF interaction energy can be decomposed as follows

$$\Delta E^{\mathrm{UHF}} = \Delta E^{\mathrm{HL}} + \Delta E_{\mathrm{def}}^{\mathrm{UHF}}, \tag{2}$$

where ΔE^{HL} is the Heitler–London (HL) energy[33,34] and $\Delta E_{\mathrm{def}}^{\mathrm{UHF}}$ represents the UHF deformation contribution. The ΔE^{HL} energy may be further divided into the first-order Hartree–Fock electrostatic $E_{\mathrm{els}}^{(100)}$ (for the perturbation terms notation, see, *e.g.*, ref.[24]) and HL exchange-penetration $\Delta E_{\mathrm{exch}}^{\mathrm{HL}}$ components

$$\Delta E^{\mathrm{HL}} = \Delta E_{\mathrm{exch}}^{\mathrm{HL}} + E_{\mathrm{els}}^{(100)}\,. \tag{3}$$

The UHF deformation energy defined by Eq. (*2*) originates from mutual electric polarisation effects and exchange effects due to the Pauli principle. An important and the simplest exchangeless approximation to $\Delta E_{\mathrm{def}}^{\mathrm{UHF}}$ is the second-order UHF Coulomb induction energy ($E_{\mathrm{ind}}^{(200)}$)[24,25,27]. It may be viewed as the classic induction effect between the permanent and induced multipole moments resulting from the polarisation of the monomer A by the permanent multipole moments of the monomer B and *vice versa*. The exchange penetration counterpart represents the $E_{\mathrm{ex\,-ind}}^{(200)}$ energy[27].

Similarly to the closed-shell cases, the second-order UMP2 correlation interaction energy can be partitioned as

$$\Delta E_{\mathrm{int}}^{(2)} = E_{\mathrm{disp}}^{(200)} + E_{\mathrm{els}}^{(12)} + \Delta E_{\mathrm{other}}^{(2)} \ . \qquad (4)$$

$E_{\mathrm{disp}}^{(200)}$ and $E_{\mathrm{ex\,-disp}}^{(200)}$ represent the second-order coulombic[26,27,35] and exchange Hartree–Fock dispersion[26,27] energies. They result from interactions of induced instantaneous electric moments. $E_{\mathrm{els}}^{(12)}$ denotes the second-order electrostatic correlation energy (containing $E_{\mathrm{els}}^{(102)}$ and $E_{\mathrm{els}}^{(120)}$ energies). It describes electrostatic interactions of the correlated multipole moments of the monomer A with uncorrelated moments of the monomer B and *vice versa*. The remaining term $\Delta E_{\mathrm{other}}^{(2)}$ encompasses the exchange and deformation correlation corrections as well as the response effects[24–27].

Using the diagrammatic techniques, it is possible to distinguish the third-order interaction energy contributions like the dispersion-correlation ($E_{\mathrm{disp}}^{(210)}$, $E_{\mathrm{disp}}^{(201)}$) and Hartree–Fock third-order ($E_{\mathrm{disp}}^{(300)}$) and fourth-order ($E_{\mathrm{disp}}^{(400)}$) dispersion energies[26,28]. However, complete physical interpretation of higher than second-order contributions of interaction electron-correlation energies is not straightforward.

CALCULATION DETAILS

All I-PT calculations were performed using our own program codes interfaced to the Gaussian 94 program package[36]. The supermolecular BSSE was determined via the counterpoise method of Boys and Bernardi[20]. The presented UHF interaction energy terms were developed using dimer-centered basis sets of the constituent monomers[21]. The HL energy was obtained using the standard Gram–Schmidt orthogonalisation procedure. All electrons were correlated in the presented calculations.

The standard polarised basis set POL reported by Sadlej and Urban[37,38] has been used for the atoms studied. It consists of the near triple-ζ quality basis set augmented by the polarisation functions optimised to reproduce

molecular electric properties, in particular polarisabilities. In order to improve the effects of the basis set on the quality of the interaction energy calculations, we have also used the modified set of the midbond functions [3s3p2d] of Tao and Pan (with the exponents 0.9, 0.3, 0.1 for sp; 0.6, 0.2 for d and 0.3 for f)[39]. These bond functions are fixed at the center of the axis defined by the H and CO centers of mass. The corresponding extended basis set is denoted as POL+bf.

A system of Jacobi coordinates (r, R, Θ) was used in all our calculations. The coordinates r, R and Θ represent the intramolecular C–O distance, the distance from H atom to the centre of mass of CO molecule, and the Jacobi angle, respectively. If this convention is used, $\Theta = 0°$ denotes the linear-orientation H–CO, while $\Theta = 180°$ designates the linear-orientation H–OC. In this work, the r distance was kept at the value of 1.128 Å (ref.[40]).

RESULTS AND DISCUSSION

Features of the PES

The two-dimensional PES (data are available on request) of the ground electronic state of the H–CO van der Waals complex was calculated in the range of R from 3.0 to 10.0 Å and Θ from 0 to 180°. The calculated potential energy points were fitted for the future use in the molecular dynamics calculations to the following general functional form

$$E_{\mathrm{int}}(R,\Theta) = \sum_{L=0}^{7} P_L^0(\cos\Theta)\left[\sum_{k=0}^{4} a_k^L\left[\exp\left(-a_1\left(R-a_2\right)\right)\right]^k + \frac{b_1^L}{r^6} + \frac{b_2^L}{r^{12}}\right], \qquad (5)$$

where $P_L^0(\cos\Theta)$ denotes a Legendre polynomial of order L. The rigorous least-square fitting procedure based on the singular value decomposition was used to determine all 58 variational parameters (Table I). Prior to the least-square calculation, the original grid of 133 calculated potential energy points have been expanded by the bicubic spline interpolation procedure[41] to 4126 points (the points above the energy of 100 μE_{h} were excluded from the calculation). The average absolute deviation of the fit was 4.1 μE_{h}. The evaluated PES reveals three stationary points (Fig. 1). The potential energy minimum occurs for a bent geometry at $\Theta = 76°$ (carbon side of the CO system) and R = 3.61 Å, and its interaction energy amounts to –156.5 μE_{h} (Table II). The linear orientations correspond to the saddle points localised at R = 4.37 Å ($\Theta = 0°$) and R = 3.91 Å ($\Theta = 180°$). The similar shape of PES

and relatively weak anisotropy in the region of bent orientation was also indicated in the cases of the interaction of CO molecule with rare gas atoms (He–CO [40], Ne–CO [42], Ar–CO [43]).

Within the supermolecular calculations, the truncation effect of the correlation treatment on the values of interaction energies is important. Its role is illustrated in Table II. The major repulsive contribution originates

TABLE I

Parameters of the analytical potential (see Eq. (*5*)) (a_1 = 1.23997, a_2 = 4.24637, all parameters are in atomic units)

L	a_0^L	a_1^L	a_2^L	a_3^L	a_4^L	b_1^L	b_2^L
0	–11.75591	–1013.46129	–248.68390	309.52089	–37.04960	–0.15397	–0.00597
1	0.79774	–405.07743	50.68797	265.16103	–53.58048	–0.04840	–0.00170
2	–2.90894	–312.52684	–356.36881	588.62144	–99.98263	–0.02756	–0.00325
3	1.56062	–87.13955	79.50010	150.42779	–33.87777	–0.00601	–0.00005
4	0.40517	–19.68653	5.37288	130.53434	–27.48882	0.00392	–0.00010
5	0.73224	–20.59330	46.05904	3.52619	–2.22304	–0.00042	0.00011
6	0.29969	–4.26760	20.87769	–7.28833	1.42606	0.00270	0.00005
7	–0.75009	18.84521	–40.59325	21.49944	–3.12704	0.00551	–0.00012

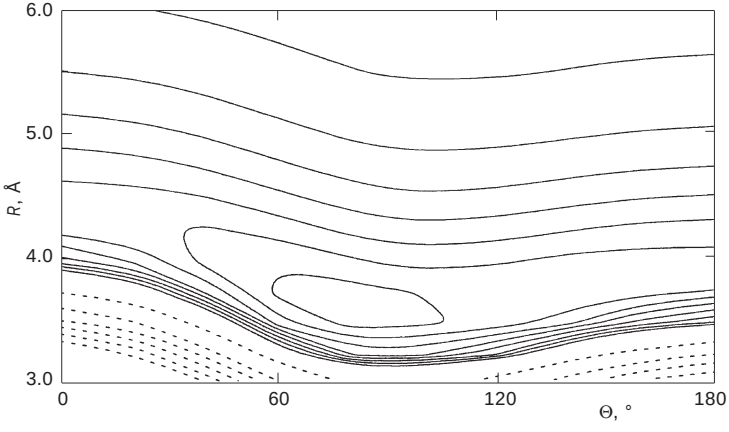

FIG. 1

Contour plot of the PES calculated at the CCSD(T)/POL+bf level of theory. The solid (dotted) lines stand for negative (positive) values of the interaction enegies. The spacing between solid (dotted) contours is 20 μE_h (250 μE_h)

from the UHF interaction energy (ΔE^{UHF}). A dominant part of the interaction correlation energy naturally originates from the values computed at the UMP2 level of theory. Despite the fact that the contributions of $\Delta E^{(3)}$ ($\Delta E^{(3)}_{int} - \Delta E^{(2)}_{int}$) and $\Delta E^{(4)}$ ($\Delta E^{(4)}_{int} - \Delta E^{(3)}_{int}$) are smaller (*ca* 10–30% with respect to the $\Delta E^{(2)}$ value), they affect the value of the interaction energies. The interaction energies calculated using the CCSD(T) method for the basis sets used

TABLE II
Individual contributions to the interaction energy (in μE_h) of the vdW H–CO complex

Energy	R = 3.61 Å, Θ = 76°		R = 3.91 Å, Θ = 180°		R = 4.37 Å, Θ = 0°	
	POL	POL+bf	POL	POL+bf	POL+bf	POL+bf
ΔE^{UHF}	181.7	177.3	97.1	94.8	124.1	127.9
$\Delta E^{(2)}$	–187.2	–261.5	–145.1	–185.6	–137.2	–184.9
$\Delta E^{(2)}_{int}$	–5.5	–84.2	–48.8	–90.8	–13.1	–57.0
$\Delta E^{(2+3)}$	–213.0	–292.7	–150.9	–191.9	155.4	–208.8
$\Delta E^{(3)}_{int}$	–31.3	–115.4	–53.8	–97.1	–31.3	–80.9
$\Delta E^{(2+3+4)}$	–238.0	–327.4	–180.1	–225.7	–181.0	–238.6
$\Delta E^{(4)}_{int}$	–56.3	–150.3	–83.0	–130.9	–56.9	–110.7
$\Delta E^{CCSD(T)}$	–242.1	–332.4	–178.9	–225.4	–183.1	–240.9
$\Delta E^{CCSD(T)}_{int}$	–60.4	–155.1	–81.8	–130.6	–59.0	–113.0
ΔE^{HL}	210.0	207.9	114.0	111.8	141.4	146.7
$E^{(100)}_{els}$	–69.8	–72.0	–52.6	–55.4	–51.6	–50.0
ΔE^{HL}_{exch}	279.8	279.9	166.6	167.2	193.0	196.7
ΔE^{UHF}_{def}	–28.3	–30.6	–16.9	–17.0	–17.3	–18.8
$E^{(200)}_{ind}$	–54.0	–55.8	–39.8	–39.7	–16.4	–16.8
$E^{(200)}_{ex\text{-}ind}$	46.6	46.9	36.2	35.9	12.3	12.3
$E^{(12)}_{els}$	–7.2	–12.0	–4.2	–10.1	–2.2	–3.5
$E^{(200)}_{disp}$	–229.0	–304.4	–181.6	–220.5	–148.1	–203.7
$E^{(200)}_{ex\text{-}disp}$	17.4	25.4	14.8	18.4	19.9	17.3
$\Delta E^{(2)}_{other}$	31.6	29.5	25.1	26.6	13.1	5.0
$E^{(210)}_{disp} + E^{(201)}_{disp}$	–21.8	–35.0	–0.2	–5.0	–21.2	–32.9
$E^{(300)}_{disp}$	1.8	12.2	0.7	5.4	1.0	8.7
$E^{(400)}_{disp}$	–12.4	–17.1	–8.0	–11.7	–7.7	–12.0

appear to be slightly deeper around the localised minima when compared with the UMP4 values. All these data clearly indicate weak bonding for the investigated complex in its electronic ground state. In order to check the sensitivity of the interaction energy to the position of the bond functions, we performed test calculations for R = 2.9 Å and Θ = 0°. Our results indicate that ±0.2 Å shifts of these functions to the C atom leads to *ca* 1% changes in interaction energies. In all cases, the spin contamination was negligible because the $\langle S^2 \rangle$ = 0.750 corresponds to the exact value in radical monomer as well as dimer.

Partitioning of Interaction Energies

The next step of this study is to discuss the physical origin of the stability of indicated vdW structures. Using the decomposition of the supermolecular UMP interaction energy, we can analyse and estimate how the fundamental components determine its anisotropy in the region near 3.6 Å. These dependences are shown in Figs 2 and 3.

The UHF interaction energies (ΔE^{UHF}) display a striking angular dependence. In the linear arrangement (Θ = 0°), the total UHF interaction energy curves show a maximum, while the second linear one (Θ = 180°) corre-

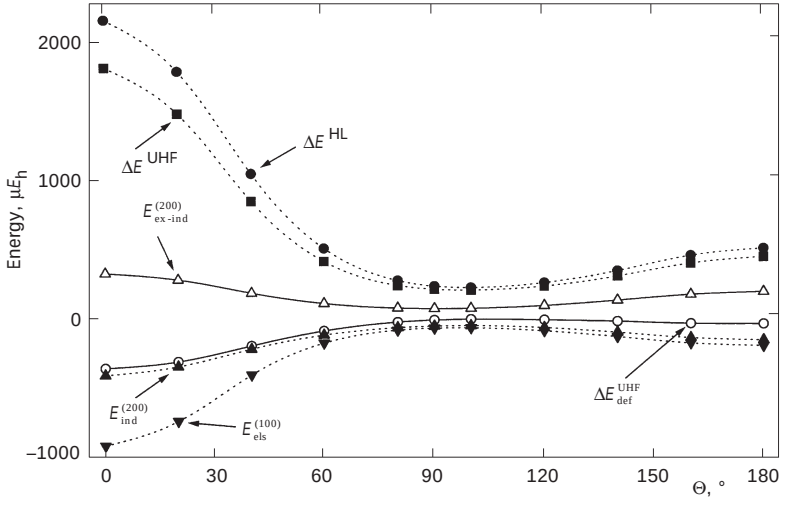

FIG. 2

Angular dependence of the HF interaction energies and their components at R = 3.6 Å (calculated in the POL+bf basis set). All energies are in μE_h. ● ΔE^{HL}, ■ ΔE^{UHF}, △ $E^{(200)}_{\mathrm{ex\text{-}ind}}$, ○ $\Delta E^{\mathrm{UHF}}_{\mathrm{def}}$, ▲ $E^{(200)}_{\mathrm{ind}}$, ▼ $E^{(100)}_{\mathrm{els}}$

sponds to a second maximum of ΔE^{UHF} (see also Table II). A minimum appears at the perpendicular geometry. The decomposition of the ΔE^{UHF} energy leads to the repulsive HL and attractive ΔE_{def}^{UHF} terms. The angular dependence of the above-mentioned terms shows also three extreme points in the investigated range. Consecutive separation of the HL energy according to Eq. (*3*) reveals that the positive value of this term comes out only from the repulsive character of the HL exchange-penetration energy contributions (ΔE_{exch}^{HL}). The attractive character of the Coulomb forces represented by $E_{els}^{(100)}$ energy evidently appears at the carbon side of CO molecule (see Fig. 2). This might be explained by stronger nuclear and mainly electron repulsion between the hydrogen atom and oxygen side of the CO system. The maximal values of these repulsion contributions appear around the perpendicular arrangement. The flattening of ΔE_{exch}^{HL} and $E_{els}^{(100)}$ angular dependence close to the oxygen atom might indicate the flattening of the diffuse part of the electron density.

The UHF deformation term (ΔE_{def}^{UHF}) has a reciprocal character to the dependence of HL energy and has a minimal effect on the total UHF interaction energy around the perpendicular configuration. The origin of the largest value of the ΔE_{def}^{UHF} energy (especially around $\Theta = 0°$) is also interesting. An important part of this energy is the UHF induction term ($E_{ind}^{(200)}$), which

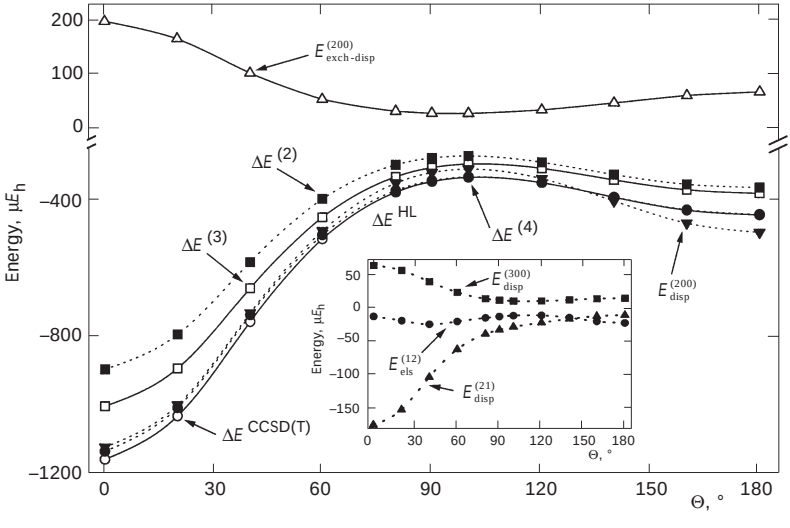

FIG. 3

Angular dependence of the interaction correlation UMP-n as well as CCSD(T) energies and their components at R = 3.6 Å (calculated in the POL+bf basis set). All energies are in μE_h. △ $E_{exch-disp}^{(200)}$, ■ $\Delta E^{(2)}$, □ $\Delta E^{(3)}$, ● $\Delta E^{(4)}$, ▼ $E_{disp}^{(200)}$, ○ $\Delta E^{CCSD(T)}$; inset: ■ $E_{disp}^{(300)}$, ● $E_{els}^{(12)}$, ▲ $E_{disp}^{(21)}$

describes the classic charge-induction. As can be seen from Fig. 2, the induction interaction between the neutral hydrogen atom and CO molecule is dominant for $\Theta < 60°$. The large differences between $E_{ind}^{(200)}$ and ΔE_{def}^{UHF} energies indicate that the repulsive exchange-induction energies play a non-negligible role in the UHF deformation energy[24,25].

The correlation components are plotted in Fig. 3. As expected, $\Delta E^{(2)}$ is important in forming the shape of the total UMP2 interaction energy curves. The $E_{disp}^{(200)}$ makes the dominant attractive contribution within the interaction correlation energy (see Table II). Similar to the case of $E_{ind}^{(200)}$ energy, the dispersion component favours linear arrangements. A comparison of the interaction energy components calculated within the POL and POL+bf basis sets shows that extension of the basis set affects primarily the dispersion energies. The remaining calculated Coulomb terms represent the electrostatic correlation energy ($E_{els}^{(12)}$). Interestingly, it has maxima at 0 and 90° and minima at 50 and 180°. It seems that the reshaping of the electron density due to the second-order correlation effects occurs mainly at the side of the carbon atom. The repulsive contributions collected in $\Delta E_{other}^{(2)}$ energy also affect the second-order interaction correlation energy $\Delta E^{(2)}$.

The higher-order dispersion corrections ($E_{disp}^{(210)}$, $E_{disp}^{(201)}$ and $E_{disp}^{(300)}$) that appear in the third-order interaction correlation energy ($\Delta E^{(3)}$) are presented in Fig. 3 and Table II. The sum of the higher-order dispersion corrections approximates very well (in both basis sets used) the third-order contribution of the interaction correlation energy around the vdW stationary point. The importance of the higher-order dispersion energies within the fourth-order interaction correlation contributions indicate the non-negligible negative values of the $E_{disp}^{(400)}$ energies (see Table II).

CONCLUSIONS

The *ab initio* potential energy surface for the H–CO interaction was evaluated at the supermolecular CCSD(T) level. The minimum occurs at bent geometry and the transition states at both the linear conformations. The angular dependence of the interaction energy at R = 4.6 Å was analysed using the I-PT. The interaction energies were separated into four fundamental components – electrostatic, exchange-penetration, induction and dispersion – which have a similar physical interpretation to those arising between the closed-shell species (see, *e.g.*, refs[26,27]). The analysis of these components reveals that the UHF interaction energies calculated around the perpendicular arrangements are practically determined by the repulsive HL energy. In both investigated geometries, the attractive $E_{disp}^{(200)}$ energy dominates

$\Delta E^{(2)}$ and the dispersion interactions play also the leading role in the $\Delta E^{(3)}$ and $\Delta E^{(4)}$ energies. However, the main stabilisation effect of $E_{\text{disp}}^{(200)}$ is slightly compensated due to the repulsive contributions included in the $E_{\text{ex-disp}}^{(200)}$ and $\Delta E_{\text{other}}^{(2)}$ energies.

The obtained PES can be used later as inputs for the modelling of dynamic processes. Furthermore, the separation of the interaction energy into fundamental parts can be also helpful for deeper understanding the physical stability as well as to test the quality of the basis set used.

This work was supported by the Slovak Scientific Grant Agency (projects No. 1/0055/03 and No. 1/0052/03). IBM Slovakia Ltd. is acknowledged for computing facilities.

REFERENCES

1. Pullumbi P., Bouteiller Y., Perchard J. P.: *J. Chem. Phys.* **1995**, *102*, 5719.
2. Kalemos A., Papakondylis A., Mavridis A.: *Chem. Phys. Lett.* **1996**, *259*, 185.
3. Tielens A. G. G. M. in: *Chemistry and Spectroscopy of Interstellar Molecules* (D. K. Bohme, E. Herbst, N. Kaifu and S. Saito, Eds), p. 237. University of Tokyo, Tokyo 1992.
4. Herbst E. in: *Dust and Chemistry in Astronomy* (T. J. Millar and D. A. Williams, Eds), p. 183. Institute of Physics, Bristol 1993.
5. Woon D. E.: *Astrophys. J.* **2002**, *569*, 541.
6. Bowman J. M., Bittman J. S., Harding L. B.: *J. Chem. Phys.* **1986**, *85*, 911.
7. Francisco J. S., Goldstein A. N., Wiliams I. H.: *J. Chem. Phys.* **1988**, *89*, 3044.
8. Dixon D. A., Feller D., Francisco J. S.: *J. Phys. Chem. A* **2003**, *107*, 186.
9. Cho S. W., Wagner A. F., Gazdy B., Bowman J. M.: *J. Chem. Phys.* **1992**, *96*, 2799.
10. Wang D., Bowman J. N.: *J. Chem. Phys.* **1994**, *100*, 1021.
11. Wang D., Bowman J. N.: *Chem. Phys. Lett.* **1995**, *235*, 277.
12. Lorenzen-Schmidt H., Perić M., Peyerimhoff S. D.: *J. Chem. Phys.* **1993**, *98*, 525.
13. Werner H. J., Bauer C., Rosmus P., Keller H. M., Stumpf M., Schinke R.: *J. Chem. Phys.* **1995**, *102*, 3593.
14. Keller H. M., Floethmann H., Dobbyn A. J., Schinke H. J., Bauer C., Rosmus P.: *J. Chem. Phys.* **1996**, *105*, 4983.
15. Bittererová M., Lischka H., Biskupič S.: *Int. J. Quantum Chem.* **1995**, *55*, 261.
16. Woon D.: *J. Chem. Phys.* **1996**, *105*, 9921.
17. Jursic B.: *J. Mol. Struct. (THEOCHEM)* **1998**, *427*, 157.
18. van Mourik T., Dunning T. H., Peterson K. A.: *J. Phys. Chem. A* **2000**, *104*, 2287.
19. Marenich A. V., Boggs J. E.: *J. Phys. Chem. A* **2003**, *107*, 2343.
20. Boys S. F., Bernardi F.: *Mol. Phys.* **1970**, *19*, 533.
21. van Duijneveldt F. B., van Duijneveldt-van de Rijdt J. G. C. M., van Lenthe J. H.: *Chem. Rev.* **1994**, *94*, 1873.
22. Čársky P., Urban M.: *Lect. Notes Chem.* **1980**, *16*, 174.
23. Hobza P., Zahradník R.: *Intermolecular Complexes*. Academia, Prague 1988.
24. Chalasiński G., Szcęśniak M. M.: *Chem. Rev.* **1994**, *94*, 1723.
25. Chalasiński G., Szcęśniak M. M.: *Chem. Rev.* **2000**, *100*, 4227.

26. Rybak S., Jeziorski B., Szalewicz K.: *J. Chem. Phys.* **1991**, *95*, 6576.
27. Jeziorski B., Moszyński R., Ratkiewicz A., Rybak S., Szalewicz K., Williams H. L. in: *Methods and Techniques in Computational Chemistry: METECC-94* (E. Clementi, Ed.), Vol. B. STEF, Cagliari 1993.
28. Laurinc V., Lukeš V., Biskupič S.: *Theor. Chem. Acc.* **1998**, *99*, 53.
29. Lukeš V., Laurinc V., Biskupič S.: *Int. J. Quantum Chem.* **1999**, *75*, 81.
30. Kvasnička V., Laurinc V., Biskupič S.: *Mol. Phys.* **1981**, *42*, 1345.
31. Čársky P., Zahradník R., Hubač I., Urban M., Kellö V.: *Theor. Chim. Acta* **1980**, *56*, 315.
32. Lukeš V., Laurinc V., Biskupič S.: *J. Comput. Chem.* **1999**, *20*, 857.
33. Löwdin P.-O.: *Adv. Phys.* **1956**, *5*, 1.
34. Visentin T., Cezard C., Weck G., Kochanski E., Padel L.: *J. Mol. Struct. (THEOCHEM)* **2001**, *547*, 209.
35. Kochanski E.: *J. Chem. Phys.* **1973**, *58*, 5823.
36. Frisch M. J., Trucks G. W., Schlegel H. B., Gill P. M. W., Johnson B. G., Robb M. A., Cheeseman J. R., Keith T., Petersson G. A., Montgomery J. A., Raghavachari K., Al-Laham M. A., Zakrzewski V. G., Ortiz J. V., Foresman J. B., Cioslowski J., Stefanov B. B., Nanayakkara A., Challacombe M., Peng C. Y., Ayala P. Y., Chen W., Wong M. W., Andres J. L., Replogle E. S., Gomperts R., Martin R. L., Fox D. J., Binkley J. S., Defrees D. J., Baker J., Stewart J. P., Head-Gordon M., Gonzalez C., Pople J. A.: *Gaussian 94*, Revision D.3. Gaussian Inc., Pittsburgh (PA) 1995.
37. Sadlej A.: *Collect. Czech. Chem. Commun.* **1988**, *53*, 1995.
38. Sadlej A., Urban M.: *J. Mol. Struct. (THEOCHEM)* **1991**, *80*, 147.
39. Tao F.-M., Pan Y.-K.: *J. Chem. Phys.* **1992**, *97*, 4989.
40. Heijmen T. G. A., Moszyński R., Wormer P. E. S., van der Avoird A.: *J. Chem. Phys.* **1997**, *107*, 9921.
41. Engels-Müllges G., Uhlig F.: *Numerical Algorithms with FORTRAN*. Springer, Berlin 1996.
42. McBane G. C., Cybulski S. M.: *J. Chem. Phys.* **1999**, *110*, 11734.
43. Kukawska-Tarnawska B., Chalasiński G., Olszewski K.: *J. Chem. Phys.* **1994**, *101*, 4964.